REPORT

CROWD DYNAMICS

Dynamic response and hydrodynamics of polarized crowds

Nicolas Bain* **and Denis Bartolo***

Modeling crowd motion is central to situations as diverse as risk prevention in mass events and visual effects rendering in the motion picture industry. The difficulty of performing quantitative measurements in model experiments has limited our ability to model pedestrian flows. We use tens of thousands of road-race participants in starting corrals to elucidate the flowing behavior of polarized crowds by probing its response to boundary motion. We establish that speed information propagates over system-spanning scales through polarized crowds, whereas orientational fluctuations are locally suppressed. Building on these observations, we lay out a hydrodynamic theory of polarized crowds and demonstrate its predictive power. We expect this description of human groups as active continua to provide quantitative guidelines for crowd management.

Mesmerizing impressions of virtually all patterns observed in bird flocks, fish schools, insect swarms, and even human crowds are effectively rendered in silico by simple algorithms (*1*, *2*). Going beyond visual impressions and predicting the collective dynamics of groups of living creatures in response to physical, social, or biological imperatives, however, remains a formidable challenge. Predictive models of collective motion have been developed following two opposite strategies. One strategy identifies local interaction rules between individuals (*3*). This method has been successful, to some extent, for some animal groups, including bird flocks (*4*–*6*), fish schools (*7*, *8*), sheep herds (*9*), and insect swarms (*10*). Determining the movement of human crowds, however, remains unsettled. Neither field measurements (*11*–*15*) nor laboratory experiments (*16*–*18*) have converged toward a robust set of interaction rules (*19*). A different strategy for predicting collective motion ignores the individual interaction rules and instead describes the large-scale motions in creature groups as spontaneous flows of active materials (*20*–*23*). Existing active hydrodynamic theories successfully account for a host of emergent patterns found in assemblies of microscopic motile bodies such as swimming bacteria (*24*, *25*), cell tissues (*26*–*28*), and synthetic self-propelled particles (*29*–*31*). The success of the hydrodynamic approach has been limited to microscopic bodies, and observations of large-scale creature groups have not been quantitatively described hydrodynamically.

To establish an active hydrodynamic description of spontaneous motion of humans, we made experimental observations of individuals in a crowd targeting the same direction. We demonstrate that information propagates over system-spanning scales in the form of hybrid waves combining density and speed fluctuations in this polarized crowd. Guided by the spectral properties of the velocity waves, we build on conservation laws and symmetry principles to construct a predictive theory of pedestrian flows without resorting to any behavioral assumption.

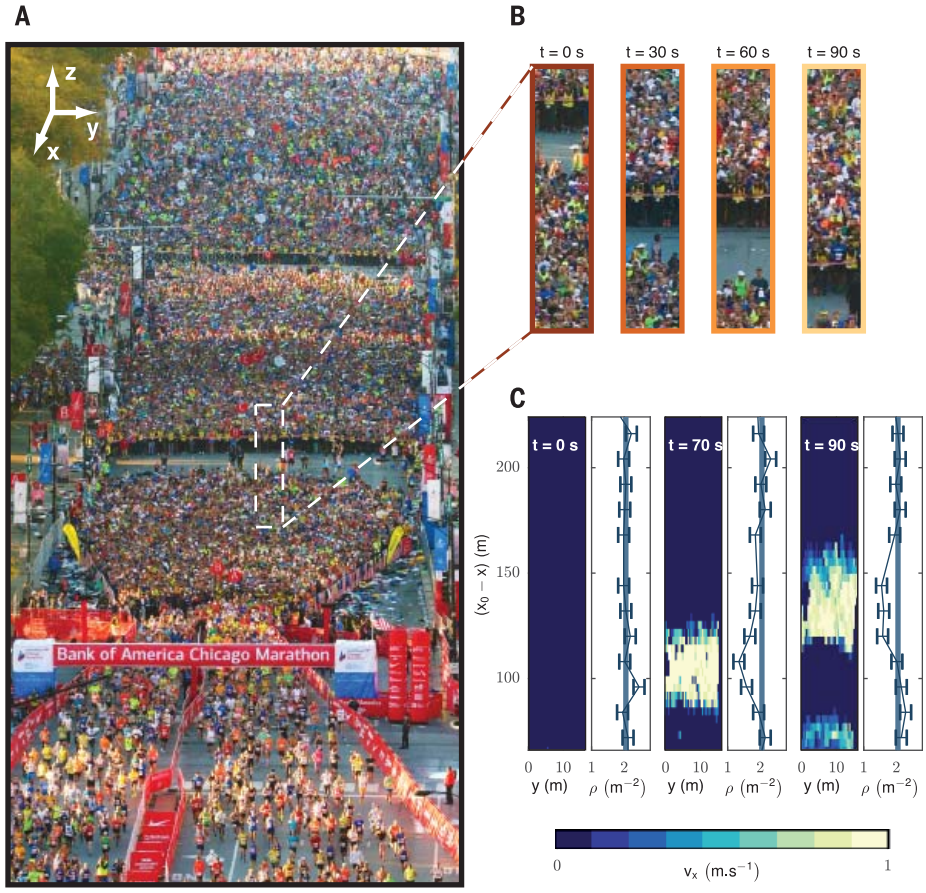

Fig. 1. Hybrid-wave propagation in queuing crowds. (**A**) Picture of the starting corrals of the Bank of America Chicago Marathon (2017) taken from an elevated observation point (*32*). Thousands of runners progress toward the starting line under the guidance of race staff members. (**B**) The chain formed by the race staff advances with repeating sequences of walks and stops. (**C**) Velocity and density fields at three successive times. At $t = 0$ s, the crowd is static and has a uniform density $\rho_0 \sim 2$ m^{-1} (blue lines). At $t > 0$, as the staff members displace the downstream boundary of the queuing crowd, a hybrid wave packet that couples velocity and density fluctuations propagates upstream. $x_0 - x$ indicates the distance from the starting line located at x_0.

A good opportunity to study a polarized crowd in a controlled setting comes from large-scale running races. We made observations of thousands of runners progressing toward the start of the Bank of America Chicago Marathon (Fig. 1A and movie S1). Starting areas of road races have a number of advantages, starting with their simple geometry. The participants are gathered in a start corral that is 200 m long and 20 m wide (Fig. 1A). The starting areas also offer the possibility to repeat observations of either the same race across several years or other races around the world. Finally, these massive polarized crowds respond to a standard excitation, as runners are consistently guided toward the starting line by staff members performing repeated sequences of walks and stops (Fig. 1, A and B).

We treated the crowd as a continuum, ignoring any specific behavior or interactions at the individual level. We characterized their large-scale motion by measuring their local density $\rho(\boldsymbol{r}, t)$ and velocity field, $\boldsymbol{v}(\boldsymbol{r}, t)$, in response to repeated translations of the boundary formed by the staff members (Fig. 1B).

At rest, we measured the density of queuing crowds to be systematically homogeneous over each entire observation window (Fig. 1C). The average density of $\rho_0 = 2.2 \pm 0.05\ \mathrm{m}^{-2}$ was remarkably identical in all corrals and varied little from one race to another (*32*). Boundary motion, however, triggers density and velocity perturbations that propagate with little attenuation over the whole extent of the corrals (Fig. 1C and movie S2). We systematically observed this coupled dynamics in response to more than 200 walk-and-stop excitations triggered by the race staff, in four different races. We gathered a total of ~150,000 individuals. The kymograph (Fig. 2A) indicates that, regardless of the width of the initial perturbation, longitudinal-velocity waves propagate upstream at a constant speed (Fig. 2B). We found that the wave speed $c_0 = 1.2 \pm 0.3\ \mathrm{m\ s}^{-1}$ is a robust characteristic of information transfer in polarized crowds for all 200 measurements. We also found that the shape of both the density and velocity waves were identical to the imposed displacements of the boundary (Fig. 2C). This faithful response to a variety of different signals (in shape and amplitude) is the signature of the propagation of nondispersive linear waves. The density and velocity waves we observed are the result of the linear response of crowds and are therefore intrinsically different from the nonlinear stop-and-go waves that have been extensively studied in pedestrian and car-traffic models; see, e.g., (*11*, *33*–*35*).

The velocity fluctuations in the crowds we observed were mainly longitudinal (Fig. 3A). This contrasts with other examples of polarized ensembles of self-propelled bodies (flocks), in which velocity fluctuations were mainly transverse (*31*, *36*). We therefore describe separately

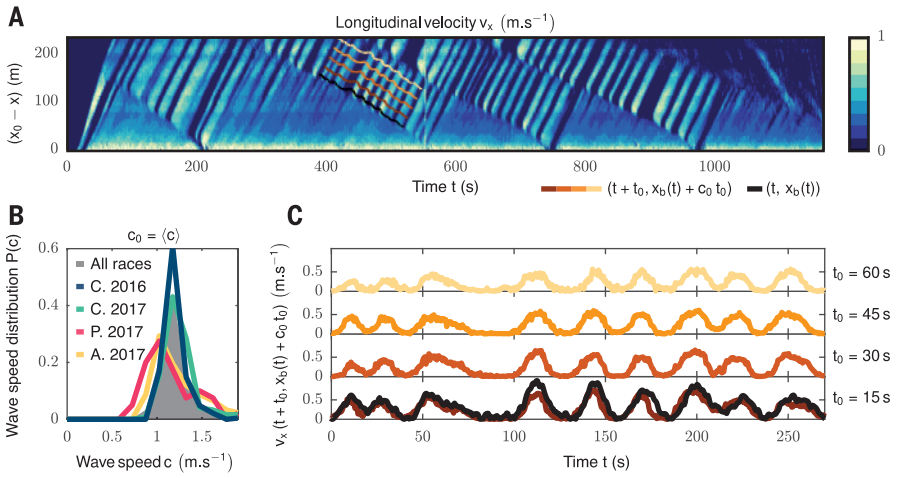

Fig. 2. Underdamped propagation of linear and nondispersive velocity waves. (**A**) Kymograph of the longitudinal velocity, averaged over the transverse direction (Chicago 2016). $x_0 - x$ indicates the distance from the starting line. A number of velocity waves are seen to propagate upstream at the same speed. (**B**) Probability distribution function of wave speed, measured for all the studied events. The typical wave speed hardly differs from one event to the other. The overall speed distribution is narrowly peaked around $\langle c \rangle = c_0 = 1.2 \pm 0.3\ \mathrm{m\ s}^{-1}$. A., Atlanta; C., Chicago; P., Paris. (**C**) Black line: velocity of a chain of race-staff members $\dot{x}_b(t)$, measured by direct tracking. The corresponding positions $x_b(t)$ are reported as a black line on the kymograph in (A). As illustrated with the same color code on the kymograph (A), the colored curves correspond to the longitudinal velocity field measured along the curves defined by the race staff position $x_b(t)$ after four different waiting times $t_0 : v_x\left(t + t_0, x_b(t) + c_0 t_0\right)$. Independently of the shape of the $\dot{x}_b(t)$ signal, the velocity waves faithfully propagate the information of the boundary speed $\dot{x}_b(t)$ over system-spanning scales, at constant speed.

the fluctuations in the speed (where $v \sim v_x$, in our case) and in the orientation, $\hat{\mathbf{v}}$, of the crowd flow. We determined the power spectrum $[C_v(\omega, q, \theta)]$ of the speed, where ω indicates the pulsation, q indicates the modulus of the wave vector, and θ indicates its orientation (*32*). We found that C_v is peaked on a straight line that defines the dispersion relation of nondispersive speed waves, $\omega = c(\theta)q$. We fitted the angular variations $[c(\theta)]$ by $c(\theta) \propto \cos\theta$, giving the dispersion relation $\omega = c_0 q_x$ with the same propagation speed c_0 as from the kymograph (Fig. 2B). This confirmed that no speed information propagated in the transverse direction to the crowd orientation (Fig. 3C). To check whether this strong anisotropy is caused by the homogeneous boundary perturbation, we analyzed separately the dynamics of freely walking crowds in the absence of guiding staff. The crowds responded to localized and spontaneous congestions forming in the starting funnel (movie S2). The corresponding power spectrum (Fig. 3B, inset) is identical to that of the runners in the crowd, establishing that polarized crowds solely support longitudinal modes. Their damping dynamics is measured from the time decay of $C_v(t, q, \theta)$ (*32*) (Fig. 3, D and E). For all wave vectors, we defined a single damping time scale α^{-1} from a best fit of the form $C_v(t, q, \theta) \sim \exp[-\alpha(q, \theta)t]\cos[c(\theta)t]$. In all cases, we found diffusively damped speed waves attenuated at a rate that scales as $\alpha(q, \theta) = D(\theta)q^2$ (Fig. 3F). Inspecting the angular variations of $D(\theta)$ (Fig. 3G), we consistently found that damping primarily occurs along the x direction as $\alpha = (D_x \cos^2\theta)q^2 = D_x q_x^2$, where the diffusivity D_x is a robust material parameter: $D_x = 1 \pm 0.5\ \mathrm{m}^2\ \mathrm{s}^{-1}$ in all observed crowds. This type of slow dynamics is usually typical of hydrodynamic variables characterized by long-lived fluctuations in the long wavelength limit (*20*, *37*). This observation is seemingly at odds with the conservation laws obeyed by pedestrian crowds. Solid friction constantly exchanges momentum between the pedestrians and the ground. Momentum is not a conserved quantity, unlike in conventional liquids. Therefore, the speed is expected to be a fast variable.

Before solving this apparent contradiction, let us address the small orientational fluctuations of pedestrian flows. The correlations of $\hat{\mathbf{v}}$, $C_{\hat{\mathbf{v}}}(t, q, \theta)$, decay exponentially in less than 2 s for all wavelengths and do not display any sign of oscillations (Fig. 3G). The corresponding damping rate $\alpha_{\hat{\mathbf{v}}}(q, \theta)$, varies as $\alpha_{\hat{\mathbf{v}}}(q, \theta) = \alpha_\perp + \mathcal{O}(q)$ (Fig. 3H). Unlike the flow speed, orientational information does not propagate in queuing crowds. Instead, it relaxes in a finite time $\alpha_\perp^{-1}$, which hardly depends on the direction of the wave vector (Fig. 3I). This behavior contrasts with that observed in bird flocks (*5*, *38*) and in all active systems in which the emergence of directed motion arises from a spontaneous symmetry breaking (*20*, *31*, *39*). In the race corrals, all participants are aware of the race direction and align their body accordingly. Rotational symmetry is explicitly broken, and no Goldstone mode exists. The $\alpha_\perp$ contribution to the damping rate stems from this

Laboratoire de Physique, ENS de Lyon, Université de Lyon, Université Claude Bernard, CNRS, F-69342 Lyon, France.
*Corresponding author. Email: nicolas.bain@ens-lyon.fr (N.B.); denis.bartolo@ens-lyon.fr (D.B.)

explicit symmetry breaking. The variations of $\alpha_{\hat{\mathbf{v}}}$ with q around $\alpha_\perp$, however, are consistent with a quadratic increase of the form $\alpha_\perp + D(\theta)q^2$ (*32*) (Fig. 3H). Such variations suggest that interactions between pedestrians penalize deformations of the flow field as would viscosity in a Newtonian fluid or orientational elasticity in polar active fluids (*36*).

The consistency between data collected from four different crowd-gathering events hints toward a unified hydrodynamic description of density and speed excitations. We elucidate the dynamical response quantified in Fig. 2 and Fig. 3 from this perspective without resorting to any behavioral assumption (*32*). Mass conservation gives the first hydrodynamic equation:

$$\partial_t \rho + \nabla \cdot (\rho \mathbf{v}) = 0 \qquad (1)$$

Momentum conservation, at lowest order in gradients, reduces to the balance between the local rate of change of momentum and the friction experienced by the crowd on the ground, $D_t[\rho(\boldsymbol{r},t)\mathbf{v}(\boldsymbol{r},t)] = \boldsymbol{F}(\{\rho\},\{\mathbf{v}\},\{\boldsymbol{p}\}) + \mathcal{O}(\nabla)$, where D_t stands for the material derivative, and the body force $\boldsymbol{F}$ is a total friction force that depends in principle on the local crowd density, velocity, and orientation (*32*). Pedestrians are polar bodies, and we classically quantify the level of local alignment between the individuals by a polarization field $\boldsymbol{p}(\boldsymbol{r},t)$ (*20*). In (*32*), we built on a systematic theoretical framework to simplify this hydrodynamic description. In short, we take advantage of three robust key observations. First, given the measured densities, the crowd is far from a jammed regime (*15*, *17*). We therefore ignore elastic stresses arising from contact interactions. Second, the local direction of the flow, $\hat{\mathbf{v}}$, quickly relaxes toward the local orientation $\hat{\boldsymbol{p}}$. Simply put, queuing pedestrians do not walk sideways. Third, the crowd is strongly polarized; all individuals align toward the $\hat{\boldsymbol{x}}$ direction. In the hydrodynamic limit, we can therefore safely assume $\hat{\boldsymbol{p}} = \hat{\mathbf{v}} = \hat{\boldsymbol{x}}$. This simplification does not allow the description of orientational fluctuations, which we explain in (*32*). It conveys, however, a clear picture of the propagation of underdamped density and speed excitations. To proceed, we need to prescribe the functional form of $\boldsymbol{F}$, which is a priori unknown but can be phenomenologically constructed in the spirit of a Landau expansion. At lowest order in gradients, the frictional body force is given by

$$\boldsymbol{F}(\{\rho\},\{\mathbf{v}\}) = -\Gamma_\parallel[\mathrm{v} - \mathrm{v}_0(\rho)]\,\hat{\boldsymbol{x}} + \mathcal{O}(\nabla) \qquad (2)$$

and represents the self-propulsion mechanism of the polarized crowd. The density-dependent speed $\mathrm{v}_0(\rho)$ quantifies the active frictional force driving the flow along $\hat{\boldsymbol{x}}$, and $\Gamma_\parallel$ is a friction coefficient that constrains the longitudinal velocity fluctuations to relax in a finite time. In the hydrodynamic limit, momentum conservation and Eq. 2 therefore reduce to the fundamental relation $\mathrm{v}(\boldsymbol{r},t) = \mathrm{v}_0\big(\rho(\boldsymbol{r},t)\big) + \mathcal{O}(\nabla)$ (*32*). This relation explains two of our main experimental findings. It shows that the fast variable v inherits the slow dynamics of the conserved density field, and it readily implies that the density of static queuing crowds self-adjusts to a constant value $\rho_0 = \mathrm{v}_0^{-1}(0)$ (Fig. 1C). In the limit of linear-response theory around the quiescent polarized state, the speed and density fluctuations, $\delta\rho$, are linearly related by $\mathrm{v}(r,t) = \mathrm{v}_0'(\rho_0)\delta\rho - (\beta/\Gamma_\parallel)\partial_x\delta\rho$, where $\mathrm{v}_0'(\rho_0) = \partial_\rho \mathrm{v}_0(\rho_0) < 0$, and β

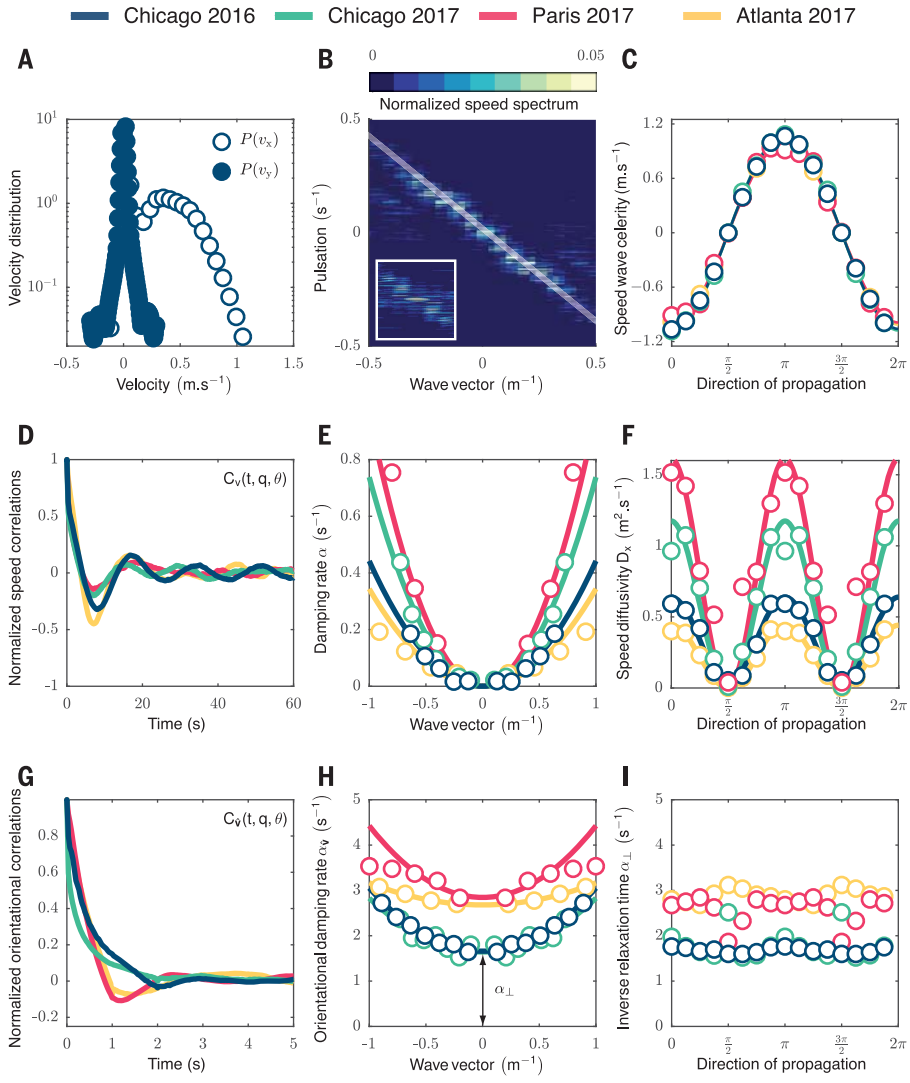

Fig. 3. Spectral properties of speed waves in queuing crowds. (**A**) Probability distribution function of the longitudinal and transverse components of the velocity field (Chicago 2016). The longitudinal component dominates. (**B**) Power spectrum of the flow speed, plotted for $\theta = \pi/4$. The spectrum is normalized at every wave vector $\left(\int C_v(\omega,q,\theta)dq = 1\right)$. The inset represents a normalized speed spectrum for a crowd in free-flow conditions. Data are from the Chicago 2016 experiment. (**C**) Variations of the celerity of the speed waves with the direction of the wave vector θ for all experiments. Circles represent experimental data. The solid line represents cosine fit. The excellent fit shows that the dispersion relation is given by $\omega = cq_x$. (**D**) Normalized speed correlations plotted versus time for all experiments ($\theta = \pi/4$, wave vector $q = 0.5\ \mathrm{m}^{-1}$). (**E**) Damping rate of the speed waves, α, plotted for all wave vectors along $\theta = \pi/4$. Circles represent experimental data. Solid lines represent best quadratic fits. (**F**) Variations of the speed diffusivity D_x with the direction of propagation. Circles represent experimental data. Solid lines represent squared cosine fits. (**G**) Normalized orientational correlations plotted versus time for all experiments ($\theta = \pi/4$, $q = 0.5\ \mathrm{m}^{-1}$). (**H**) Damping rate of the orientational fluctuations $\alpha_{\hat{\mathbf{v}}}$ plotted as a function of the wave vector ($\theta = \pi/4$). Circles represent experimental data. Solid lines represent best quadratic fits $\sim\alpha_\perp + D_{\hat{\mathbf{v}}}q^2$, with $D_{\hat{\mathbf{v}}} = 1.2 \pm 0.5\ \mathrm{m}^2\ \mathrm{s}^{-1}$. (**I**) Inverse relaxation time $\alpha_\perp$ plotted as a function of the direction of the wave vector θ. No significant angular variation is observed.

is the crowd longitudinal compressibility (32). Together with mass conservation, this constitutive relation defines the analog of the Navier-Stokes equations for polarized crowds:

$$\partial_t v + \rho_0 v_0'(\rho_0)\partial_x v - \frac{\rho_0 \beta}{\Gamma_\parallel}\partial_x^2 v = 0 \qquad (3)$$

Equations 1 and 3 effectively predict the dynamical response we observed in our experiments. The linear stability analysis of Eqs. 1 and 3 readily shows that polarized crowds support unidirectional and nondispersive speed wave propagating downstream at a speed $c_0 = -\rho_0 v_0'(\rho_0)$. Equations 1 and 3 also predict that their damping rate varies as q_x^2, in agreement with our experimental measurements (Fig. 3, E and F). Unlike in conventional fluids, the (weak) attenuation of the speed waves does not originate from viscous stresses but instead from the competition between substrate friction and compressive stresses in the crowd. In agreement with our observations, these hybrid waves coupling density and speed fluctuations of opposite amplitude are the sole propagating modes supported by polarized crowds. In the hydrodynamic limit, the response of polarized crowds is strongly unidirectional, and speed information neither propagates nor diffuses along the transverse direction (*32*).

From a more practical perspective, we can infer the full set of hydrodynamic parameters of Eq. 3 from the spectral properties of v. We can show the predictive power of our hydrodynamic model, as calibrating the celerity of the speed waves and the damping rate on a single race in Paris is sufficient to quantitatively predict the dynamics of queuing crowds observed in Chicago and Atlanta months later. In addition, our description of crowds as active continua provides effective guidelines for the management of crowds. For instance, we show that stimulations from side boundaries are inefficient and that optimal information transfer is achieved when guiding a crowd from its forefront. We show that reorienting the direction of motion of a polarized crowd at once is impossible when relying only on locally accessible signals. Orientational cues must be provided to the entire assembly to change its direction of motion. We also predict the time it takes to set in motion, or to stop, a crowd of a given extent by providing information at its boundary. Beyond these predictions, the description of crowds as continua should be useful to elucidate their response to large-amplitude perturbations and their transitions from flowing liquids to amorphous solids, two situations where crowd dynamics become hazardous.

REFERENCES AND NOTES

1. C. W. Reynolds, *ACM SIGGRAPH Computer Graphics*, vol. 21 (ACM, 1987), pp. 25–34.
2. D. Helbing, P. Molnár, *Phys. Rev. E Stat. Phys. Plasmas Fluids Relat. Interdiscip. Topics* **51**, 4282–4286 (1995).
3. T. Vicsek, A. Zafeiris, *Phys. Rep.* **517**, 71–140 (2012).
4. A. Cavagna, I. Giardina, *Annu. Rev. Condens. Matter Phys.* **5**, 183–207 (2014).
5. A. Cavagna, I. Giardina, T. S. Grigera, *Phys. Rep.* **728**, 1–62 (2017).
6. D. J. Pearce, A. M. Miller, G. Rowlands, M. S. Turner, *Proc. Natl. Acad. Sci. U.S.A.* **111**, 10422–10426 (2014).
7. J. Gautrais *et al*., *PLOS Comput. Biol.* **8**, e1002678 (2012).
8. U. Lopez, J. Gautrais, I. D. Couzin, G. Theraulaz, *Interface Focus* **2**, 693–707 (2012).
9. F. Ginelli *et al*., *Proc. Natl. Acad. Sci. U.S.A.* **112**, 12729–12734 (2015).
10. A. Attanasi *et al*., *PLOS Comput. Biol.* **10**, e1003697 (2014).
11. D. Helbing, A. Johansson, H. Z. Al-Abideen, *Phys. Rev. E Stat. Nonlin. Soft Matter Phys.* **75**, 046109 (2007).
12. M. Moussaïd, D. Helbin, G. Theraulaz, *Proc. Natl. Acad. Sci. U.S.A.* **108**, 6884–6888 (2011).
13. J. L. Silverberg, M. Bierbaum, J. P. Sethna, I. Cohen, *Phys. Rev. Lett.* **110**, 228701 (2013).
14. I. Karamouzas, B. Skinner, S. J. Guy, *Phys. Rev. Lett.* **113**, 238701 (2014).
15. A. Bottinelli, D. T. J. Sumpter, J. L. Silverberg, *Phys. Rev. Lett.* **117**, 228301 (2016).
16. M. Moussaïd *et al*., *PLOS Comput. Biol.* **8**, e1002442 (2012).
17. J. M. Pastor *et al*., *Phys. Rev. E Stat. Nonlin. Soft Matter Phys.* **92**, 062817 (2015).
18. K. W. Rio, G. C. Dachner, W. H. Warren, *Proc. Biol. Sci.* **285**, 20180611 (2018).
19. E. Cristiani, B. Piccoli, A. Tosin, *Multiscale Modeling of Pedestrian Dynamics*, vol. 12 (Springer, 2014).
20. M. C. Marchetti *et al*., *Rev. Mod. Phys.* **85**, 1143–1189 (2013).
21. R. L. Hughes, *Annu. Rev. Fluid Mech.* **35**, 169–182 (2003).
22. R. Ni, J. G. Puckett, E. R. Dufresne, N. T. Ouellette, *Phys. Rev. Lett.* **115**, 118104 (2015).
23. R. Ni, N. T. Ouellette, *Phys. Biol.* **13**, 045002 (2016).
24. H. Wioland, F. G. Woodhouse, J. Dunkel, J. O. Kessler, R. E. Goldstein, *Phys. Rev. Lett.* **110**, 268102 (2013).
25. H. H. Wensink *et al*., *Proc. Natl. Acad. Sci. U.S.A.* **109**, 14308–14313 (2012).
26. G. Duclos *et al*., *Nat. Phys.* **14**, 728–732 (2018).
27. T. B. Saw *et al*., *Nature* **544**, 212–216 (2017).
28. S. Banerjee, K. J. C. Utuje, M. C. Marchetti, *Phys. Rev. Lett.* **114**, 228101 (2015).
29. A. Zöttl, H. Stark, *J. Phys. Condens. Matter* **28**, 253001 (2016).
30. A. Morin, D. Bartolo, *Phys. Rev. X* **8**, 021037 (2018).
31. D. Geyer, A. Morin, D. Bartolo, *Nat. Mater.* **17**, 789–793 (2018).
32. Materials and methods are available as supplementary materials.
33. D. Helbing, A. Johansson, J. Mathiesen, M. H. Jensen, A. Hansen, *Phys. Rev. Lett.* **97**, 168001 (2006).
34. Y. Sugiyama *et al*., *New J. Phys.* **10**, 033001 (2008).
35. A. Tordeux, G. Costeseque, M. Herty, A. Seyfried, *SIAM J. Appl. Math.* **78**, 63–79 (2018).
36. J. Toner, Y. Tu, *Phys. Rev. E Stat. Phys. Plasmas Fluids Relat. Interdiscip. Topics* **58**, 4828–4858 (1998).
37. P. M. Chaikin, T. C. Lubensky, *Principles of Condensed Matter Physics* (Cambridge Univ. Press, 2000).
38. A. Cavagna *et al*., *Phys. Rev. Lett.* **114**, 218101 (2015).
39. J. Toner, Y. Tu, S. Ramaswamy, *Ann. Phys.* **318**, 170–244 (2005).

ACKNOWLEDGMENTS

We thank D. Reithoffer for help with the Chicago Marathon's observations and W. T. M. Irvine and E. R. Dufresne for valuable comments and suggestions. **Author contributions:** D.B. designed the research. D.B. and N.B. designed the experiments. N.B. performed the experiments and measurements. D.B. and N.B. performed the theory, analyzed and discussed the results, and wrote the paper. **Competing interests:** We declare no competing interest. **Data and materials availability:** The data that support the plots within this paper and other findings of this study are available from the corresponding authors upon request.

SUPPLEMENTARY MATERIALS

www.sciencemag.org/content/363/6422/46/suppl/DC1
Materials and Methods
Supplementary Text
Movies S1 to S3
References (*40*–*48*).

25 June 2018; resubmitted 21 July 2018
Accepted 9 November 2018
10.1126/science.aat9891

Dynamic response and hydrodynamics of polarized crowds

Nicolas Bain and Denis Bartolo

Science **363** (6422), 46-49.
DOI: 10.1126/science.aat9891

A crowd that flows like water

The behavior of large numbers of insects, animals, and other flocks is often based on rules about individual interactions. Bain and Bartolo applied a fluid-like model to the behavior of marathon runners as they walked up to the start line of the Chicago Marathon (see the Perspective by Ouellette). They observed nondamping linear waves with the same speed for different starting corrals of runners and at different races around the world. Their model should apply both to this type of polarized crowd as well as to other groups, which may help guide crowd management.

Science, this issue p. 46; see also p. 27